

Electron-deuteron tensor polarization and the two-nucleon force

M. I. Haftel,* L. Mathelitsch, and H. F. K. Zingl

Institut für Theoretische Physik, Universität Graz, A-8010 Graz, Austria

(Received 10 September 1979)

Electron-deuteron scattering observables, including the tensor polarizations T_{20} , $T_{2\pm 1}$, $T_{2\pm 2}$, are calculated for a variety of N - N potential models. The main goal is to determine how the tensor polarization experiments can help distinguish competing potential models with respect to off-shell behavior and tensor force strength. The pair meson-exchange-current correction of Gari and Hyuga is included in the analysis as well as a correction suggested by Friar for energy-dependent potentials. It is found that whereas electron-deuteron elastic scattering cross sections do not readily distinguish different potentials, the tensor polarizations do. The tensor polarization T_{20} mainly distinguishes potentials with different deuteron s -wave momentum distributions, but does not distinguish potentials with different d -state probabilities (P_D). The tensor polarization $T_{2\pm 1}$, since it factors essentially into a product of the magnetic and quadrupole form factors, allows for the extraction of the quadrupole form factor which is closely related to the tensor force strength and P_D . The tensor polarization $T_{2\pm 2}$ is completely determined by the elastic scattering cross sections and magnetic form factor, and yields no additional information on the N - N force unobtainable from elastic scattering measurements. The tensor polarizations T_{20} and T_{21} have maximum values of order unity in the region $q = 2$ to 5 fm^{-1} . The calculations indicate that measurements of T_{20} for $2 \lesssim q \lesssim 5 \text{ fm}^{-1}$, and $T_{2\pm 1}$ for $3 \lesssim q \lesssim 5 \text{ fm}^{-1}$ could yield important information on the off-shell behavior and tensor force strength. The meson-exchange-current and energy-dependence corrections are important and must be taken into account to extract potential properties from such experiments.

NUCLEAR STRUCTURE ^2H : form factors, tensor polarization calculated; dependence on off-shell behavior and P_D ; seven potential models; pair currents included.

I. INTRODUCTION

One of the main hopes of electron-deuteron (e - d) scattering experiments has been to "measure" certain features of the deuteron wave function and relate these to determining unknown properties of the nucleon-nucleon force. In particular, one would like to employ e - d scattering to help pinpoint the nature of the short-range repulsion and the tensor force strength.^{1,2} These features are undetermined even after forty years work on the N - N force as evidenced by the fact that the current literature contains competing potential models with strong local short-range repulsion,^{3,4} "supersoft" local repulsion,⁵ and "soft" nonlocal repulsion.⁶⁻⁸ An even more disconcerting unknown is the tensor force strength, as indicated by the uncertainty in the deuteron d -state probability P_D (3-7%).⁹ Despite these differences, these competing models all give good fits to the existing N - N data¹⁰; however, the uncertainties in the short-range repulsion can lead to sizable uncertainties in nuclear matter predictions¹¹ and nuclear electromagnetic form factors (at medium to high q^2),¹² while the uncertainty in P_D is more serious, even affecting static few-nucleon properties such as the triton binding energy.¹³ The aforementioned uncertainties exist even for potentials de-

rived from meson theory (for example, compare the s - and d -wave coordinate and momentum space wave functions² of the Paris¹⁴ and Bonn¹⁵ potentials).

One source of the incomplete knowledge of the N - N force comes from the fact that phase shifts are known over only a finite energy range (0-600 MeV).¹⁰ However, even if phases were known to all energies, one can use the "off-shell" freedom (by using unitary transformations,¹¹ for example) to show that the phases alone determine uniquely neither the potential nor the wave functions at short distances (or equivalently, in momentum space language, the off-shell T matrix elements). It is here that electron scattering experiments become most useful since they measure largely the charge and magnetic densities of nuclei, quantities very closely related to the entire wave function, whereas N - N scattering experiments measure only the asymptotic wave function. The main purpose of this paper is to indicate how e - d tensor polarization measurements can help distinguish different nuclear force models especially with respect to the short-range (or "off-shell") behavior and tensor force strength.

Electron-deuteron elastic scattering cross sections depend on the electric form factor [$A(q)$] and magnetic form factor [$B(q)$]. These form fac-

tors, in turn, depend on the monopole (or charge) [$F_C(q)$], quadrupole [$F_Q(q)$], and magnetic [$F_M(q)$] structure functions of the deuteron,¹⁶ i.e., integrals involving the s - and d -wave components of the deuteron wave function and the momentum transfer q . The cross sections measure the combination (Ref. 17) $A(q) + B(q) \tan^2 \theta/2$, where $A(q)$ depends on all three structure functions, $B(q)$ depends only on $F_M(q)$, and θ is the scattering angle of the electron in the lab system. Therefore it is possible to separate $B(q)$ from $A(q)$ by measuring angular distributions [and so determine $F_M(q)$], but $F_C(q)$ cannot be separated from $F_Q(q)$. This leads to a major difficulty in using e - d cross sections to differentiate nuclear potential models; competing potential models, which differ greatly in the behavior of the s -wave function [which influences mainly $F_C(q)$], and also differ greatly in the d -wave function [which influences P_D and $F_Q(q)$], can give similar values for the experimentally measurable quantity $A(q)$, at least for low and moderate q^2 ($q^2 \lesssim 25 \text{ fm}^{-2}$).^{1,2,18} An example of this is given in Sec. V of this paper. Moreover, $F_C(q)$ and $F_Q(q)$ separately are more potential dependent than $A(q)$,^{2,18} hence it is desirable to be able to measure these individually. True, $F_M(q)$ can give further information about the deuteron wave function. However, $F_M(q)$ is slightly less sensitive to changes in the potential model than $F_C(q)$ or $F_Q(q)$, and is not sensitive to the tensor force. It is also related to the wave function (and interaction) in a more complicated way.² In this paper we mainly concentrate on the charge scattering (but we do not ignore the magnetic scattering).

Of course, cross-section measurements are not the only experimental possibility. As of yet unperformed tensor polarization experiments afford the opportunity of measuring observables that depend on different combinations of F_C , F_Q , and F_M , thus enabling us to separate F_C and F_Q and better rule on nuclear potentials.^{1,2} The idea of using tensor polarization to help determine the N - N force is not new. Schildknecht and Gourdin¹⁹ wrote down the relations of the tensor polarization quantities to the deuteron wave functions in 1964. Levinger¹ suggested tensor polarization measurements to learn about the unknown features of the N - N interaction. Since then several investigators have calculated the polarization P (related to the T_{20} of this paper) for different potential models.^{1,2,20-22} Only recently, however, have the experiments at the interesting values of q^2 ($q^2 \gtrsim 4 \text{ fm}^{-2}$) become feasible, and now the linacs at Saclay and M.I.T.-Bates seem logical facilities to perform such experiments.²³

This paper examines the dependence of tensor

polarization quantities on the choice of the N - N interaction. We choose the potential models in such a way as to assess how tensor polarization separately measures the effects of changing the s -wave momentum distribution (or off-shell behavior),²⁴ which mainly affects $F_C(q)$, from the tensor force strengths, which affects P_D and shows up in $F_Q(q)$. We consider the tensor polarization quantities T_{20} , $T_{2\pm 1}$, and $T_{2\pm 2}$ (Ref. 25) instead of only the previously considered T_{20} . While $T_{2\pm 2}$ does not yield any new information [it is proportional to $F_M(q)$], the previously unconsidered $T_{2\pm 1}$ essentially measures $F_Q(q)$ and thus is a most convenient quantity to measure the tensor force properties.

In our calculations of tensor polarization we include the pair meson-exchange-current (MEC) correction of Gari and Hyuga since these are the most important for $F_C(q)$ and $F_Q(q)$ in the momentum transfer region considered.^{26,27} Since the MEC are model dependent, they should be considered in assessing the model dependence of the total scattering process. Other MEC corrections are important in the magnetic scattering,²⁶ but since magnetic scattering plays a relatively minor role in our analysis, we ignore them. Other relativistic corrections^{22,28-31} are not included, but the reader should be aware that they are not negligible even at $q^2 = 10 \text{ fm}^{-2}$. The relativistic corrections and excluded MEC mainly affect the high momentum components of the wave function and the form factors at large q^2 (although they can change static properties, like the deuteron magnetic moment μ_D). One main point of our paper is that tensor polarization quantities readily distinguish between potential models even for q^2 between 4 and 16 fm^{-2} , where these corrections should not be overly large.

In Sec. II of this paper we express the e - d scattering observables ($d\sigma/d\Omega$, T_{20} , $T_{2\pm 1}$, $T_{2\pm 2}$) in terms of structure functions which are, in turn, related to the deuteron wave function.^{19,25} While T_{20} is a rather complicated combination of F_C , F_Q , and F_M , $T_{2\pm 1}$ and $T_{2\pm 2}$ have relatively simple expressions. $T_{2\pm 2}$ is simply proportional to $F_M^2(q)$, while $T_{2\pm 1}$ is proportional to $F_M F_Q$. Since F_M can be measured by backward angle cross sections, we have the important result that $T_{2\pm 1}$ is a direct measure of F_Q , hence closely related to the tensor force and P_D , whereas $T_{2\pm 2}$ does not yield any new information about the deuteron wave function. In Sec. III we describe the potential models we consider. We choose two potentials with rather strong short-range repulsion (Bonn³² and Reid⁴) but with different tensor force properties ($P_D = 4.4$ and 6.5%, respectively). We also consider a pair of potentials of Doleschall (D4 and D7)⁸ as

examples of potentials with "soft" separable short-range repulsion and again varying P_D (4% vs 7%). Therefore, we are in a position to compare potentials with nearly the same off-shell behavior but varying P_D (Reid vs Bonn, D4 vs D7) and also potentials of nearly the same P_D but varying off-shell behavior (Reid vs D7, Bonn vs D4). We also consider the Graz,⁷ Paris,³³ and Nijmegen³⁴ potentials as further examples.

In Sec. IV we describe the form factor calculations both with and without the MEC. We also consider, for the Bonn potential, corrections to the form factors, suggested by Friar,⁴⁹ originating from the energy dependence of this potential. This correction is fairly large. We present the structure functions calculated for the various potential models, and the influence of the MEC. For both F_C and F_Q the MEC are model dependent in such a way as to reduce, but not eliminate, the potential dependence of these form factors. One important influence of the MEC is that for F_Q the MEC corrections depend mainly on the s -wave momentum distribution, thus disturbing somewhat the correlation between F_Q and P_D discussed by Mathelitsch and Zingl.²

Section V presents the e - d observable calculations. We first survey $A(q)$ for the various potentials in comparison with the experimental data.³⁵ Usually $A(q)$ cannot distinguish between potentials as well as F_C and F_Q separately. Five of the seven potentials studied (all except the Doleschall pair) fit the experimental data very well up to $q^2 \approx 35$ fm⁻² when the pair MEC is included. The tensor polarization T_{20} rather clearly differentiates models of different off-shell behavior even in those cases where $A(q)$ does not. Furthermore, such differences appear even around $q = 2$ fm⁻¹ where T_{20} is large (≈ 1.0). However, T_{20} does not distinguish different P_D values, at least where the magnitude of T_{20} is appreciable. The tensor po-

larization $T_{2\pm 1}$ has qualitatively similar features to T_{20} with a maximum value of ~ 0.5 at $q \approx 3$ to 5 fm⁻¹. Since $T_{2\pm 1}$ provides a rather direct measurement of $F_Q(q)$, and F_Q is related to P_D , we discuss in some detail the usefulness of measuring $T_{2\pm 1}$ to determine P_D . For both T_{20} and $T_{2\pm 1}$ the MEC are important to take into account. Generally, they narrow somewhat the model dependence of the tensor polarization results. Ignoring them would lead to extracting erroneous information about the deuteron wave function. Likewise, ignoring the energy-dependence correction of Friar⁴⁹ for the Bonn potential would also be misleading. Finally we caution the reader that the state of the art of MEC corrections does not presently allow a precise calculation of their contribution. Our treatment of MEC is to indicate roughly how large they *may* be and that their understanding is essential in analyzing e - d scattering experiments.

II. ELECTRON-DEUTERON SCATTERING OBSERVABLES

As is well known, the e - d scattering cross section is given by¹⁷

$$\begin{aligned} \frac{d\sigma}{d\Omega} &= \left(\frac{d\sigma}{d\Omega} \right)_{\text{MOTT}} \left[A(q) + B(q) \tan^2 \frac{\theta}{2} \right] \\ &\equiv \left(\frac{d\sigma}{d\Omega} \right)_{\text{MOTT}} N. \end{aligned} \quad (1)$$

The form factors A and B are expressed in terms of deuteron structure functions by¹⁶

$$\begin{aligned} A(q) &= F_C^2(q) + \frac{8}{9} \eta^2 F_Q^2(q) + \frac{2}{3} \eta F_M^2(q), \\ B(q) &= \frac{4}{3} \eta(1 + \eta) F_M^2(q), \end{aligned} \quad (2)$$

where $\eta = q^2/4M_D$ and M_D is the deuteron mass. The charge (F_C), quadrupole (F_Q), and magnetic (F_M) form factors are given by^{2,19}

$$F_C(q) = [G_{Ep}(q) + G_{En}(q)] \int_0^\infty r^2 dr [\psi_0^2(r) + \psi_2^2(r)] j_0\left(\frac{qr}{2}\right), \quad (3a)$$

$$\left(\frac{e}{9}\right)^{1/2} \eta F_Q(q) = 2[G_{Ep}(q) + G_{En}(q)] \int_0^\infty r^2 dr \psi_2(r) \left[\psi_0(r) - \frac{\psi_2(r)}{\sqrt{8}} \right] j_2\left(\frac{qr}{2}\right), \quad (3b)$$

$$\begin{aligned} F_M(q) &= 2[G_{Mp}(q) + G_{Mn}(q)] \int_0^\infty r^2 dr \left[\left(\psi_0^2(r) - \frac{\psi_2^2(r)}{2} \right) j_0\left(\frac{qr}{2}\right) + \left(\frac{1}{\sqrt{2}} \psi_0(r)\psi_2(r) + \frac{1}{2} \psi_2^2(r) \right) j_2\left(\frac{qr}{2}\right) \right] \\ &\quad + \frac{3}{2} [G_{Ep}(q) + G_{En}(q)] \int_0^\infty r^2 dr \psi_2^2(r) \left[j_0\left(\frac{qr}{2}\right) + j_2\left(\frac{qr}{2}\right) \right], \end{aligned} \quad (3c)$$

where ψ_0 , ψ_2 are the s - and d -wave deuteron wave functions and G_{Ep} , G_{En} , G_{Mp} , G_{Mn} are the proton and neutron electric and magnetic form factors in the usual notation. The form factors F_C , F_Q ,

and F_M represent Fourier transforms of the electric monopole, quadrupole, and magnetic dipole densities, respectively, in the Breit frame. Strictly speaking, one must add the MEC con-

tributions to these operators to the respective form factors.

One separates $B(q)$ from $A(q)$ [and hence determines $F_M(q)$] from backward angle scattering cross sections.¹⁷ However, the elastic scattering cross sections cannot distinguish $F_C(q)$ from $F_Q(q)$. This is a major drawback in employing e - d scattering to learn about the N - N force. $F_C(q)$ contains information mainly of the off-shell behavior (or s -wave momentum distribution, see Ref. 24), while $F_Q(q)$ is mainly sensitive to the strength of the tensor force and is closely related to P_D . Clearly F_C and F_Q could be such that potentials with very different F_C and F_Q separately conspire to give almost the same $A(q)$ (we give an example of where this actually happens in Sec. V). At low q , $F_M(q)$ is sensitive to mainly the same features as $F_C(q)$ but at intermediate and high q it is not as potential sensitive.² Furthermore, it is not too sensitive to the tensor force and also is more obscurely related to the deuteron wave function [see Eq. (3c)]. Obviously it is important to be able to determine $F_C(q)$ and $F_Q(q)$ individually.

Since the deuteron is a $s=1$ system, tensor (and vector) polarizations are also observables that could be measured. Since vector polarization is down by a factor M_e/M_p ,¹⁹ we consider only tensor polarizations. These observables, which involve different combinations of F_C , F_Q , and F_M than the cross sections, in principle, can separate the effects of these three form factors. Following Schildknecht¹⁹ and the Madison convention²⁵ the expressions for T_{20} , $T_{2\pm 1}$, and $T_{2\pm 2}$ are

$$T_{20} = -(\sqrt{2} N)^{-1} \left\{ \frac{8}{9} \eta^2 F_Q^2 + \frac{8}{3} \eta F_C F_Q + \frac{2}{3} \eta F_M^2 \left[\frac{1}{2} + (1 + \eta) \tan^2(\theta/2) \right] \right\}, \quad (4a)$$

$$T_{2\pm 1} = (\sqrt{2} N)^{-1} [\pm 2\eta(\epsilon - \eta) \tan(\theta/2) F_M F_Q], \quad (4b)$$

$$T_{2\pm 2} = -\eta F_M^2 / (2\sqrt{3} N), \quad (4c)$$

$\epsilon = |\vec{p}|/M_D$, where \vec{p} is the incident electron momentum.

The tensor polarization T_{20} involves a rather complicated combination of F_C , F_Q , and F_M . For the momentum transfers considered in this paper, and at nonbackward angles, the terms involving F_M are not important. In principle, measurements of $A(q)$, $B(q)$, and T_{20} are sufficient to determine F_C , F_Q , and F_M . However, since experimental errors are finite, it is desirable to investigate numerically the sensitivity of T_{20} and $T_{2\pm 1}$ to changes in F_C and F_Q individually, as is the procedure in this work.

The heretofore largely ignored tensor polariza-

tion $T_{2\pm 1}$ is interesting in that it factors into the products of the magnetic and quadrupole form factors. The magnetic form factor, of course, can be extracted from backward angle cross sections. Therefore, by measuring $T_{2\pm 1}$ and dividing through by the known magnetic form factor (and multiplying by N , which is also known) one can directly extract F_Q . Therefore measurements of $T_{2\pm 1}$ can yield rather important information concerning the tensor force and P_D . In Sec. V we discuss how useful $T_{2\pm 1}$ is in determining the tensor force strength as contained in P_D . The tensor polarization $T_{2\pm 2}$ does not yield any information not obtainable from backward angle cross sections since it only depends on F_M^2 . If for some reason, however, it is easier to measure the ratio $T_{20}/T_{2\pm 2}$ than to measure T_{20} itself, knowing the ratio is tantamount to knowing T_{20} itself since $T_{2\pm 2}$ is already known from the magnetic form factor. (The same applies to extracting $T_{2\pm 1}$.) Actual calculations³⁶ of $T_{2\pm 2}$ indicate that this ratio is roughly 60 at $q=0$ and decreases to about 25 at $q=5 \text{ fm}^{-1}$. Having now described how tensor polarization may be used to help determine the N - N force, we now describe the actual potential models employed.

III. POTENTIALS AND WAVE FUNCTIONS

In our investigation of deuteron tensor polarization we employ seven potential models of the N - N force: the Reid soft core (RSC),⁴ the Bonn (α -dependent) potential (B),³² two potentials of Doleschall⁸ (D4 and D7, differing in $P_D=4\%$ and 7% , respectively), the Paris (P),³³ Graz (G),⁷ and Nijmegen (N) (Ref. 34) potentials. The Bonn, Paris, and Nijmegen potentials are derived from meson theory. The Bonn potential has an energy dependence which results from a field theoretic Hamiltonian which includes one and two boson exchange. The Reid potential is phenomenological, but has a one-pion-exchange (OPE) tail. The Doleschall and Graz potentials are separable. All potentials give at least qualitative fits to the N - N data up to 300 MeV, but are not phase-shift equivalent. The non-phase equivalence is not critical since the electron scattering probes the interior wave functions and this is related closer to the so-called off-shell behavior²⁴ of the force rather than the phase shifts. Nevertheless, the static properties of the deuteron, which do affect the e - d scattering results, do depend on the on-shell properties at low energies, and these are listed in Table I.

The rationale for our choice of the potentials is as follows. We would like to determine the separate effects of changing the s -wave off-shell (or

TABLE I. Static properties of the deuteron.

	a (fm)	r_0 (fm)	E_D (MeV)	Q (fm ²)	A_s	η
D4	a	a	2.2250	0.285	0.790	0.0265
D7	a	a	2.2250	0.285	0.743	0.0190
RSC	5.397	1.720	2.2246	0.280	0.878	0.0262
B	5.43	1.77	2.2260	0.271	0.905	0.0255
P	5.471	1.808	2.2245	0.278	0.887	0.0264
G	5.445	1.80	2.2245	0.287	0.887	0.0340
N	5.489	1.846	2.2246	0.286	0.900	0.0263

^aNot calculated.

momentum) dependence and of changing the tensor force (or P_D) in e - d scattering results. A useful parameter² in describing the off-shell behavior is p_* , the value of the momentum at which the s -wave momentum space wave function passes through zero. Another parameter in describing the off-shell behavior² is P_{HE} , which is defined²

$$P_{HE} = \int_{p_*}^{\infty} p^2 dp \psi_0^2(p)$$

and is a measure of the "high energy component" of the deuteron wave function. Generally nuclear structure calculations (binding energies, spectra, etc.) are more sensitive to p_* than to P_{HE} .^{37,38} However, form factors at large q^2 and nuclear matter calculations are also sensitive to P_{HE} . Furthermore, if the high energy component of the deuteron wave function could be experimentally determined, it could help judge between the various approaches of deriving the N - N interaction from meson theory.³⁹ In this investigation we primarily focus on the p_* parameter. For the tensor force strength we adhere to the traditional choice of P_D as the parameter of importance. Table II lists p_* , P_{HE} , and P_D for the potentials of our study. The reader should note that RSC and B have very similar p_* (but different P_{HE}) but varying P_D , and the same is true of D4 and D7. Likewise, the B and D4 pair, and the RSC and D7 pair, both have P_D 's that vary only by $\frac{1}{2}\%$ yet

TABLE II. p_* , P_{HE} , P_D for the different potentials.

	p_* (fm ⁻¹)	P_{HE} (%)	P_D (%)
D4	2.85	0.11	4.00
D7	2.70	0.27	7.00
RSC	1.97	0.79	6.47
B	2.04	0.43	4.40
P	2.15	a	5.45
G	∞	0	2.63
N	1.97	0.29	5.39

^aNot calculated.

have quite different values of p_* . Therefore, we are in a position to examine separately the effects of varying P_D and p_* . The Graz, Paris, and Nijmegen potentials are employed for further comparison, but most of our comparisons will involve RSC, B, D4, and D7.

Before proceeding to describing our calculations of e - d scattering quantities, we plot in Figs. 1 and 2 the s - and d -wave configuration space wave functions of our study. Figures 3 and 4 show the corresponding momentum space wave functions. The difference between potentials show up most dramatically in s waves at distances $r < 0.7$ fm, where differences between hard, soft, and "soft" nonlocal repulsion greatly affect the amount of suppression in the wave function. In momentum space the difference between a "hard" and "soft" local repulsion (compare RSC, B, and P) does not show up very much at all until $p \approx 3$ fm⁻¹, although the potentials with soft nonlocal repulsion do differ (for s waves) even at $p \approx 1.5$ fm⁻¹. For s waves all potentials are virtually the same up to $p \approx 1.5$ fm⁻¹, evidencing the similarities in their long range or static properties. Additional variations show up in d -wave functions because of the different normalizations (i.e., P_D is different). One might question the type of the behavior of the Doleschall potentials since they are separable and do not have explicit OPE tails. True, most potentials derived from meson theory give $p_* \approx 2$ fm⁻¹.⁴⁰ This, however, is not an explicit constraint of such potentials, and one such potential, the Paris (75) potential,¹⁴ gives s -wave momentum space wave functions fairly similar to the Doleschall pair. So we should consider p_* a parameter that should be experimentally determined. Finally we submit that the parameter p_* and P_D are not just of academic interest. Nuclear matter predictions are very sensitive to both p_* (Ref. 11) and P_D ,⁴¹ and even the properties of light nuclei, such as the triton binding energy, are slightly sensitive to p_* and rather sensitive to P_D .^{12,13,38}

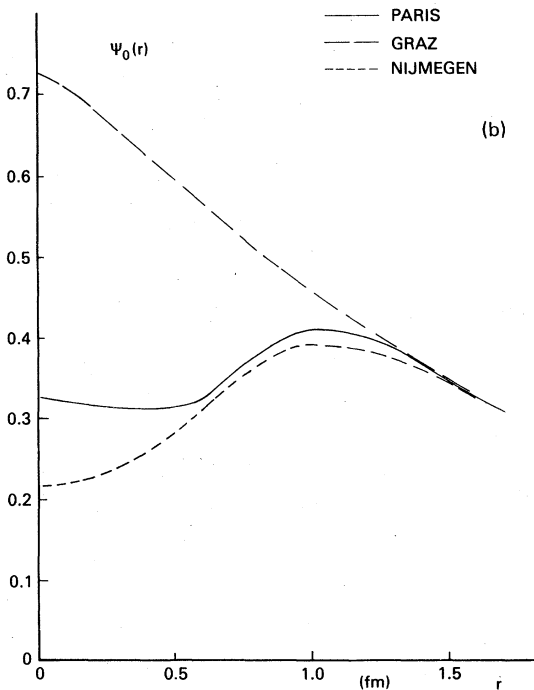
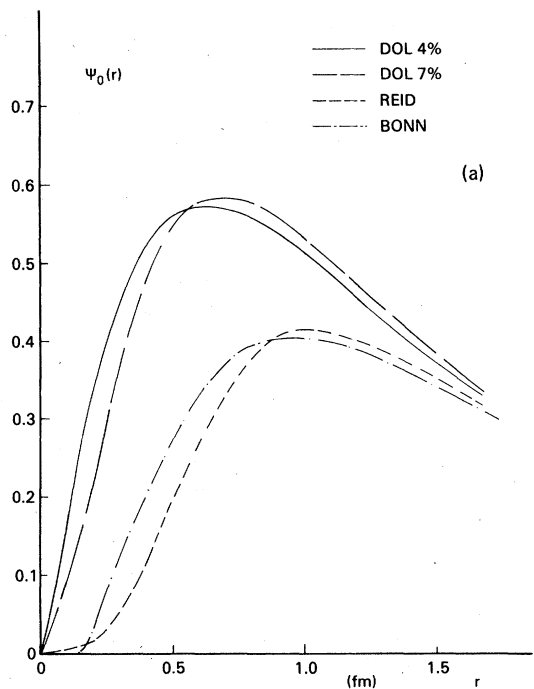


FIG. 1. s -wave functions in configuration space (a) for the Doleschall $D4$ and $D7$, Reid SC, and Bonn potentials and (b) for the Paris, Graz, and Nijmegen potentials.

IV. FORM FACTOR CALCULATIONS

Expressions for the form factors $A(q)$, $B(q)$ in terms of F_C , F_Q , and F_M , as well as F_C , F_Q , and

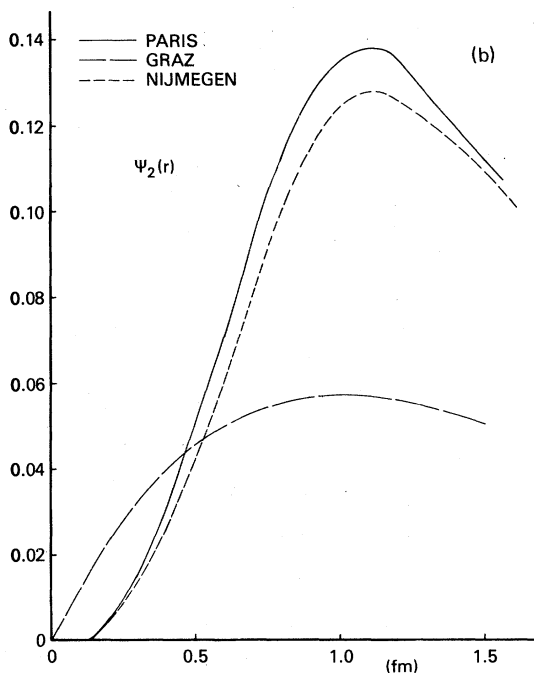
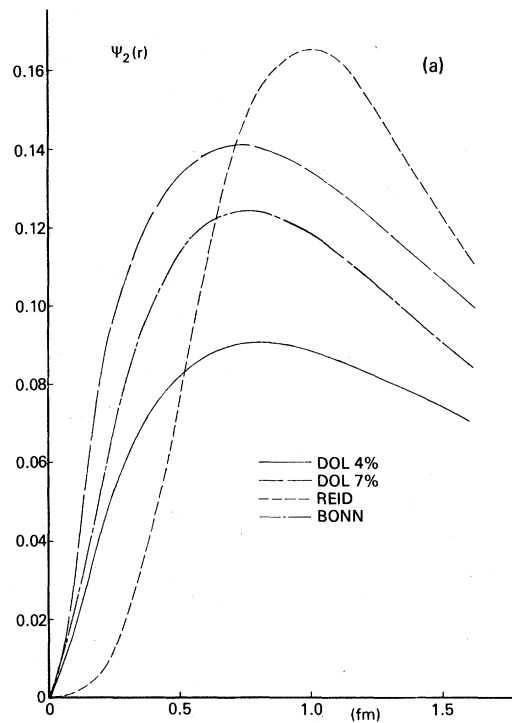


FIG. 2. d -wave functions in configuration space (a) for the potentials in Fig. 1(a) and (b) for the potentials in Fig. 1(b).

F_M in terms of the deuteron wave function have been discussed in Sec. II. Expressions for these form factors in terms of momentum space wave functions have been given by Mathelitsch and

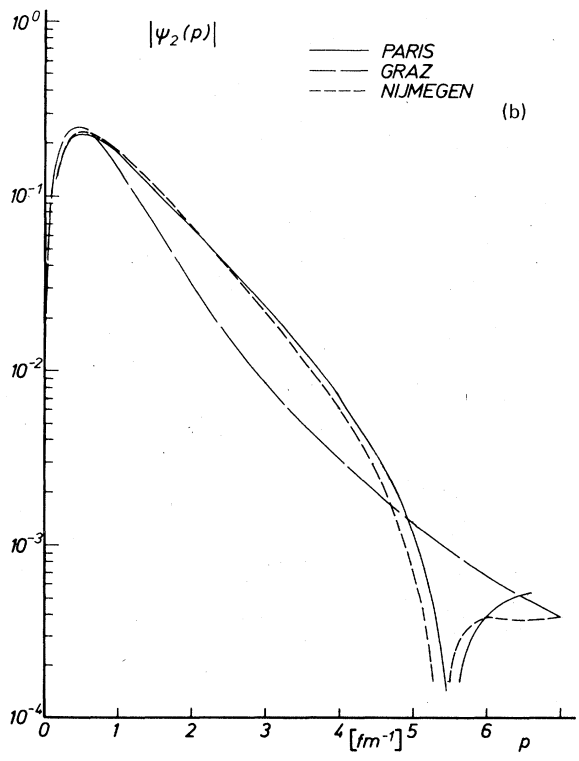
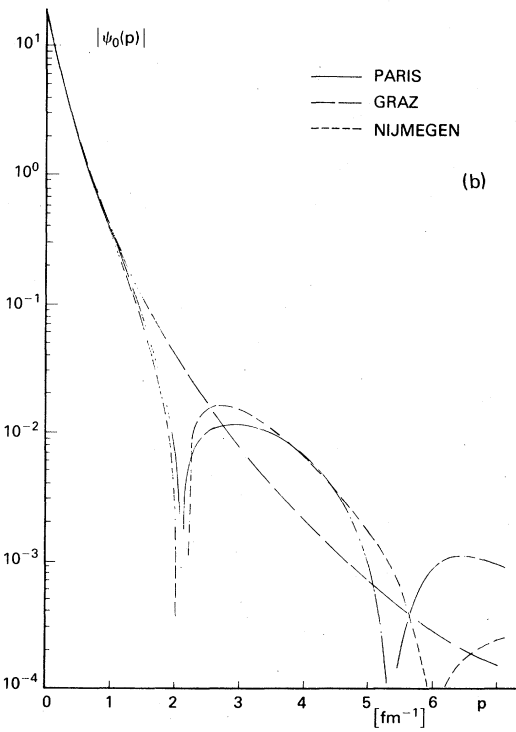
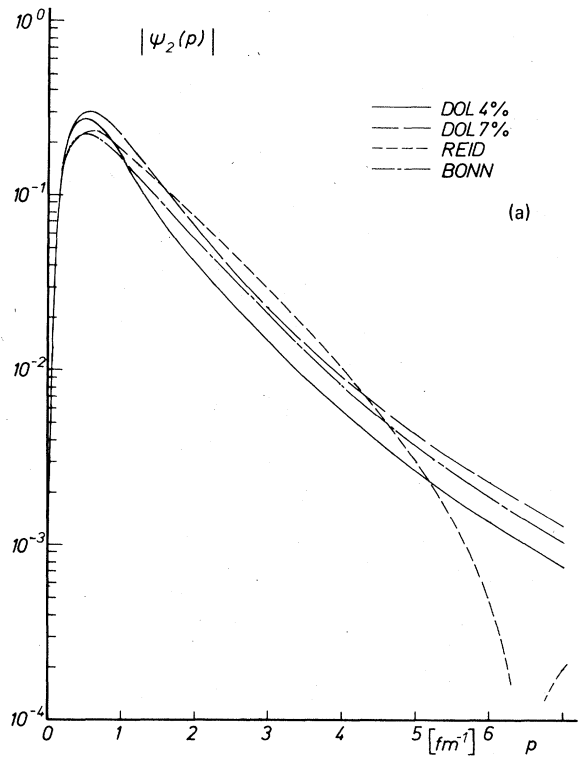
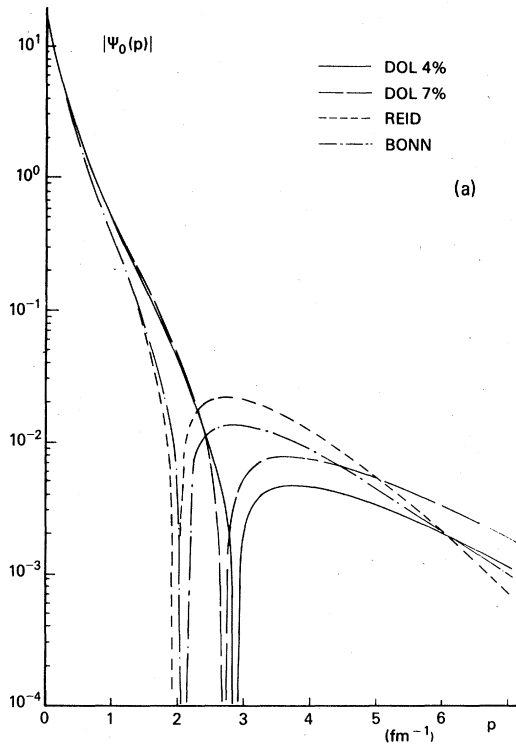


FIG. 3. *s*-wave functions in momentum space (a) for the potentials in Fig. 1(a) and (b) for the potentials in Fig. 1(b).

FIG. 4. *d*-wave functions in momentum space (a) for the potentials in Fig. 1(a) and (b) for the potentials in Fig. 1(b).

Zingl.² The present calculations employ integrals evaluated in r space for the local potentials (RSC, P) and p -space wave functions for the rest. We use the dipole nucleon form factors, i.e.,

$$\begin{aligned} G_{Ep}(q) &= (1 + q^2/18.235 \text{ fm}^{-2})^{-2}, \\ G_{En}(q) &= 0, \\ G_{Mp}(q) &= \mu_p G_{Ep}(q), \\ G_{Mn}(q) &= \mu_n G_{Ep}(q), \end{aligned} \quad (5)$$

where μ_p and μ_n are the proton and neutron magnetic moments in nuclear magnetons. The difference in deuteron form factor results between the dipole nucleon form factors and the parametrization of Iachello, Jackson, and Landé (IJL)⁴² has been discussed by Gari and Hyuga.²⁶ Generally, the difference is only a few percent for $q^2 \leq 20 \text{ fm}^{-2}$, but greater at larger q^2 . Interestingly, the uncertainty for $q^2 \leq 20 \text{ fm}^{-2}$ is even smaller if MEC are included.

Even for $q^2 \leq 20 \text{ fm}^{-2}$ MEC are significant. For the momentum transfers under consideration we assume that the "pair current" is the most important for F_C and F_Q .^{26,27} Gross⁴³ has demon-

strated that for pseudoscalar coupling the standard MEC calculations (including "pair," "recoil," and renormalization effects) are consistent with his relativistic deuteron theory to order M^{-3} . Gari and Hyuga²⁷ demonstrate that the recoil and renormalization effects cancel in the nonrelativistic limit for $F_M(q)$, but are of the same order [$O(M^{-3})$] for F_C and F_Q . In this work we consider only the pair contributions and do not consider the recoil and renormalization effects. Our preliminary calculation of the recoil and renormalization effect shows it to be 1–20% of the pair term, but model dependent even with respect to the sign. The ρ - ω MEC is important^{26,44} for the magnetic form factor in this region whereas the pair current gives a relatively small correction to $F_M(q)$. At $q^2 \leq 20 \text{ fm}^{-2}$ and at forward angles F_M plays a very small role in $A(q)$ and T_{20} . In $T_{2\pm 1}$, F_M does play an important role, but we emphasize that the main utility in measuring $T_{2\pm 1}$ is to divide by an experimentally known F_M to get F_Q , in which case the MEC corrections to F_M become irrelevant. With the MEC of Gari and Hyuga, the pair current corrections to F_C , F_Q , and F_M are given by^{26,45}

$$F_C^\pi(q) = -\frac{g_{\pi NN}^2}{16M^3\pi^2} [G_{Mp}(q) + G_{Mn}(q)] q \int_0^\infty k^2 dk \{ [\frac{1}{2} q \mathcal{G}_0^\pi(k, q) + k \mathcal{G}_1^\pi(k, q)] [I_{000}(k) + I_{202}(k)] + [q \mathcal{G}_2^\pi(k, q) + 2k \mathcal{G}_3^\pi(k, q)] [-2\sqrt{2} I_{022}(k) + I_{222}(k)] \}, \quad (6a)$$

$$\begin{aligned} \frac{2\sqrt{2}}{3} \eta F_Q^\pi(q) &= \frac{g_{\pi NN}^2}{4\sqrt{2}\pi^2 M^3} [G_{Mp}(q) + G_{Mn}(q)] q \int_0^\infty k^2 dk \{ [\frac{1}{2} q \mathcal{G}_0^\pi(k, q) + k \mathcal{G}_1^\pi(k, q)] [I_{000}(k) + \frac{1}{10} I_{202}(k)] \\ &+ \frac{1}{\sqrt{2}} [\frac{1}{2} q \mathcal{G}_2^\pi(k, q) + k \mathcal{G}_3^\pi(k, q)] I_{022}(k) \\ &+ \frac{11}{88} [\frac{1}{2} q \mathcal{G}_2^\pi(k, q) + \frac{28}{55} k \mathcal{G}_3^\pi(k, q) + \frac{27}{55} k \mathcal{G}_3^\pi(k, q)] I_{222}(k) \\ &+ \frac{54}{35} [\frac{1}{2} q \mathcal{G}_4^\pi(k, q) + k \mathcal{G}_3^\pi(k, q)] I_{242}(k) \}, \end{aligned} \quad (6b)$$

$$\begin{aligned} F_M^\pi(q) &= -\frac{g_{\pi NN}^2}{8M^3\pi^2} [G_{Mp}(q) + G_{Mn}(q)] \int_0^\infty dk k^2 \{ \{ k^2 [\mathcal{G}_0^\pi(k, q) - \mathcal{G}_2^\pi(k, q)] [I_{000}(k) - \frac{1}{2} I_{202}(k)] \\ &- \{ k^2 [\mathcal{G}_0^\pi(k, q) - \mathcal{G}_2^\pi(k, q)] + \frac{9}{20} qk [\mathcal{G}_1^\pi(k, q) - \mathcal{G}_3^\pi(k, q)] \} \\ &\times [\sqrt{2} I_{022}(k) + I_{222}(k)] \}, \end{aligned} \quad (6c)$$

where $g_{\pi NN}$ is the pion-nucleon coupling constant, M is the nucleon mass, $\mathcal{G}_i^\pi(k, q)$ are the pion currents given by Gari and Hyuga,²⁶ and

$$I_{lnl}(k) \equiv \int_0^\infty r^2 dr \psi_l(r) \psi_{l'}(r) j_n(kr). \quad (7)$$

In calculating $\mathcal{G}_i^\pi(k, q)$ we use the monopole vertex function which, in the notation of Gari and Hyuga, is

$$K_{\pi NN}(q^2) = (1 + q^2/\alpha^2)^{-1}$$

with $\alpha = 5.3160 \text{ fm}^{-1}$.

Before discussing the structure functions and scattering observables, we address two important points. First, the "standard" approach to MEC, including ours, is an *ad hoc* one. One is presented a prescription for the MEC contributions to the electromagnetic (em) operators which contains certain assumptions concerning the N - N potential (especially the OPE part). These assumptions are not necessarily consistent with the potentials under consideration. Of course in our study, which includes purely phenomenological as well as meson-exchange potentials, one is forced to such an ap-

proach. However, a better approach would be to treat the potential and electromagnetic operators in a consistent manner—say from a reduction of the Bethe-Salpeter equation with both strong and em interactions.⁴⁶ In this case the MEC operators themselves would have additional potential dependence. Conceivably these corrections could either overwhelm or completely cancel the differences between potentials for e - d observables that occur in the impulse approximation. A first calculation in this direction by Tjon and Zuilhof⁴⁶ suggests that the situation is not that pessimistic as they find that standard MEC calculations are probably overestimates of the true MEC contributions.

The second point concerns the corrections to the em operators due to wave function nonorthonormality resulting from energy-dependent potentials, such as the Bonn potential. According to Friar⁴⁹ the simplest way to handle this is to let

$$\psi^2 \rightarrow \left(1 + \frac{\partial V(E)}{\partial E}\right) \psi^2 \quad (8)$$

in the calculation of form factors, with the required renormalization. This correction is similar in character to the recoil current. At the end of this section and in the next one we consider this correction for the Bonn potential. To simplify the calculation we include only the π and σ exchange parts of the Bonn potential, whose momentum dependence (but not energy dependence) we treat in the static limit.

We now proceed to discuss the structure functions calculated for each of our models with and without the pair MEC correction. Figure 5 illustrates $F_C(q)$ for the different potentials in the impulse approximation (IA). Immediately one can see that F_C distinguishes potentials with different p_+ values quite well, but not different values of P_D . A diffraction structure appears with the diffraction minimum being correlated with the p_+ value; in fact, as previously pointed out by Mathelitsch and Zingl,² the point of the diffraction minimum (q_0) is related (in the impulse approximation) to p_+ by $q_0 \approx 2p_+$. Unfortunately, this diffraction structure does not appear in the observable quantity $A(q)$ because it is "washed out" by the quadrupole form factor contribution. The diffraction structure, however, does appear in ^3He and ^3H because, as these are $s = \frac{1}{2}$ nuclei, there is no electric quadrupole contribution. In fact, the diffraction minimum in $F_C(^3\text{He})$, $F_C(^3\text{H})$, and in $F_C(^2\text{H})$ are also correlated, and if there were no such thing as possible $3N$ forces and MEC then ^3He and ^3H would provide "looking glasses" at $F_C(^2\text{H})$. When MEC are included in F_C , as shown in Fig. 6, q_0 is decreased for all potentials and

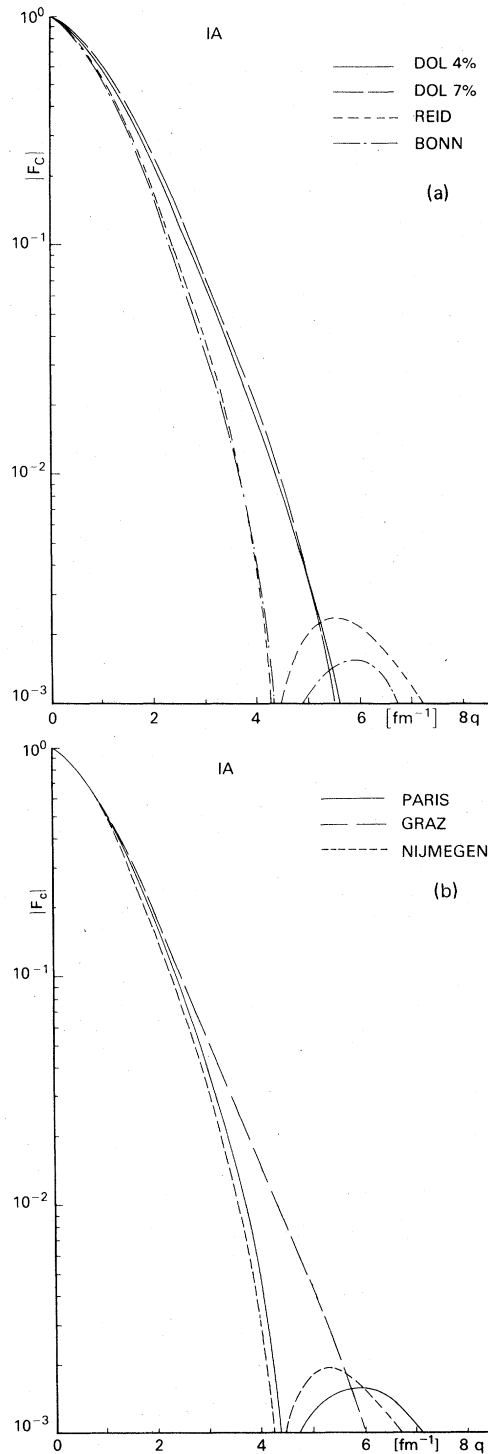


FIG. 5. $F_C(q)$ in the impulse approximation (a) for the potentials in Fig. 1(a) and (b) for the potentials in Fig. 1(b).

the height of the second maximum is increased. Jackson *et al.*⁴⁷ have previously noted this and the similarity between the MEC effects in $F_C(^2\text{H})$ and $F_C(^3\text{He})$. [If one wants a looking glass into $F_C(^2\text{H})$

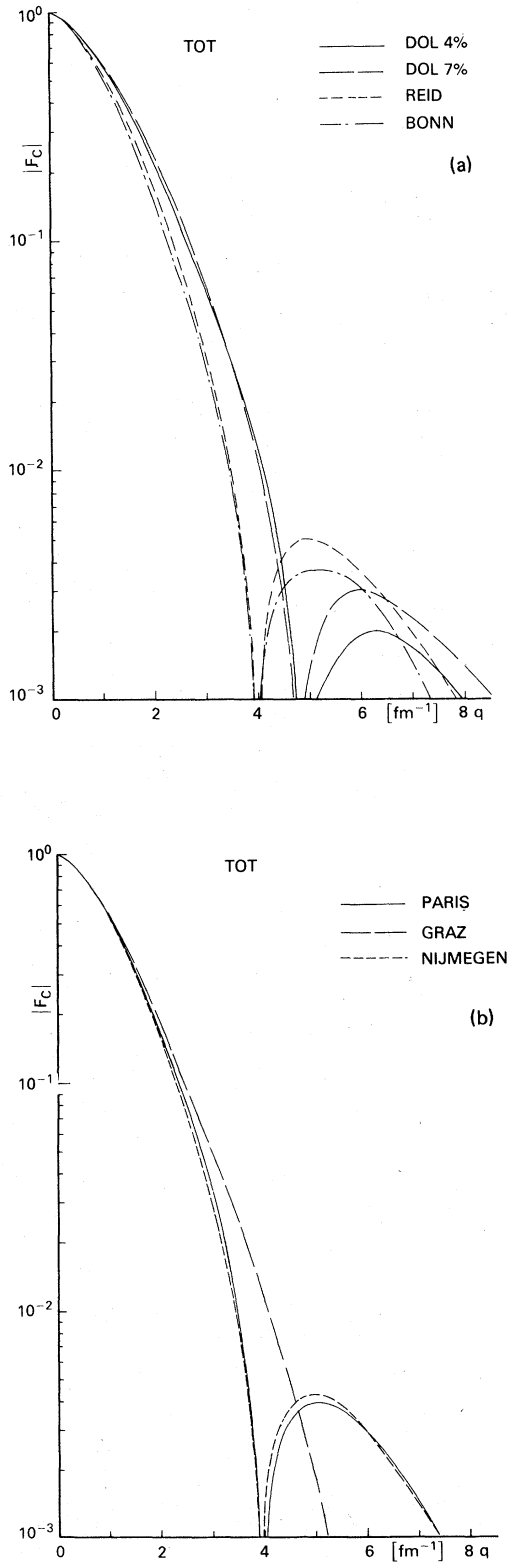


FIG. 6. $F_C(q)$ with MEC included (a) for the potentials in Fig. 1(a) and (b) for the potentials in Fig. 1(b).

in the IA, $F_C(^3\text{H})$ is better than $F_C(^3\text{He})$ because the MEC are smaller.^{18]} The model dependence of F_C is slightly less with the MEC than without, but the narrowing of the range of results does not appear as great as in ^3He .^{18]} The potential dependence of the MEC contribution to F_C (F_C^E) appears in Fig. 7. Generally speaking, softer potentials give a larger F_C^E , but the true dependence seems to depend in a somewhat complicated manner on both the off-shell behavior and the d wave (e.g., D4 and RSC give similar F_C^E). The MEC also reduce the model dependence of the height of the second maximum which, in the IA, primarily reflects the high energy component. Figure 8 illustrates $F_Q(q^2)$ in the IA. At low q^2 this form factor is $\sim Q_D \cdot q^2$, where Q_D is the deuteron quad-

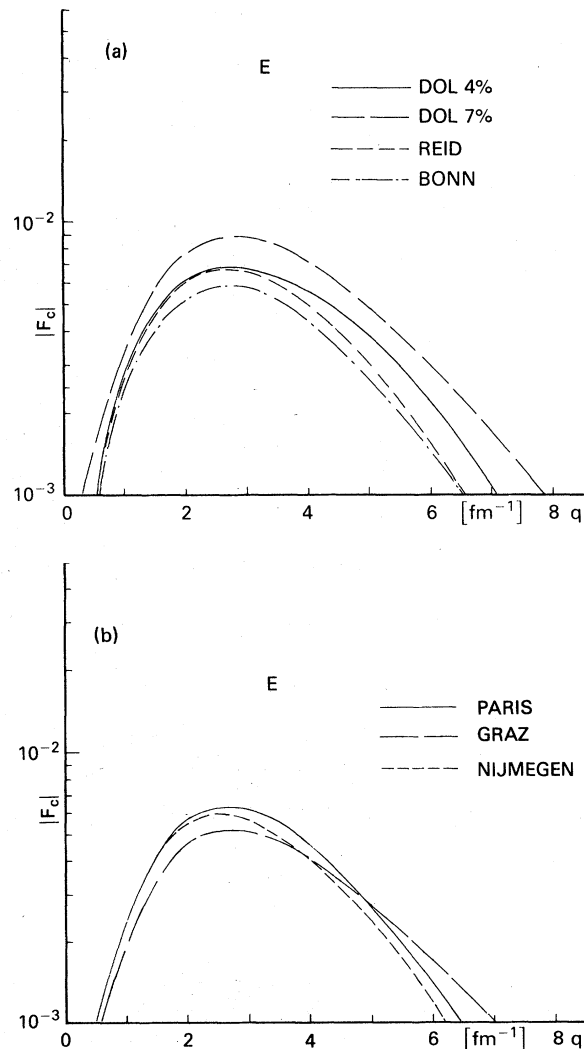


FIG. 7. MEC contribution to $F_C(q)$ (a) for the potentials in Fig. 1(a) and (b) for the potentials in Fig. 1(b). ("E" in all the figures stands for exchange currents).

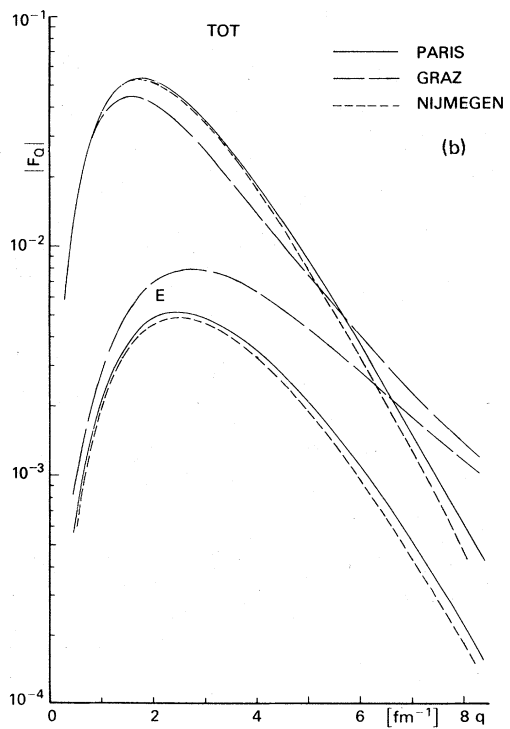
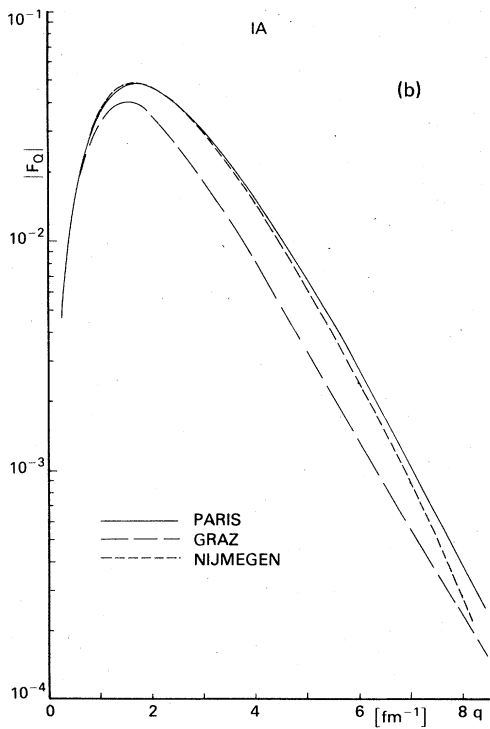
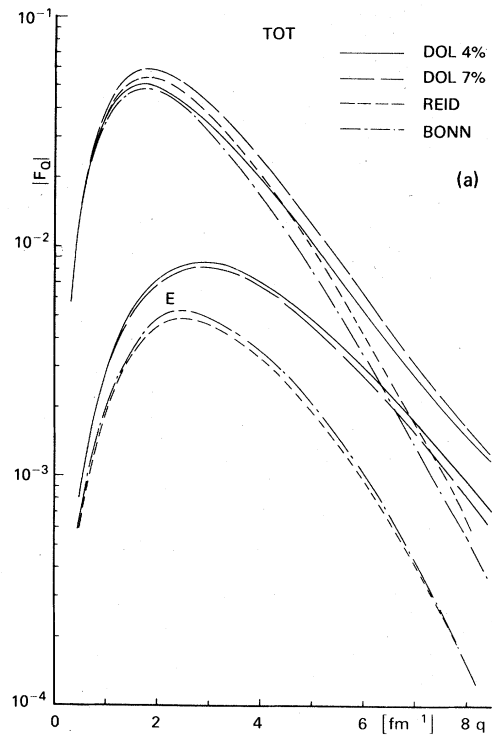
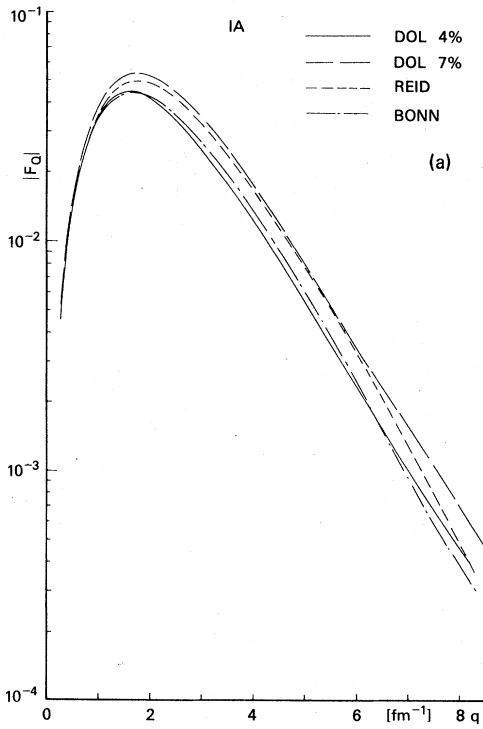


FIG. 8. $F_Q(q)$ in the impulse approximation (a) for the potentials in Fig. 1(a) and (b) for the potentials in Fig. 1(b). [F_Q plotted is $(\frac{8}{9})^{1/2}\eta F_Q$ of text.]

FIG. 9. $F_Q(q)$ with MEC included (a) for the potentials in Fig. 1(a) and (b) for the potentials in Fig. 1(b).

rupole moment. Hence, all potentials are similar. For $q \geq 1.5 \text{ fm}^{-1}$, and especially for $q > 2 \text{ fm}^{-1}$, $F_Q(q)$ starts to become model dependent and in the region $q = 2.5$ to 4 fm^{-1} appears to scale with P_D . Mathelitsch and Zingl have discussed extensively the relation of P_D and $F_Q(q)$ especially with regard to the peak in $F_Q(q)^2$. The fact that B and D4 have almost exactly the same peak value of $F_Q(q)$ despite a P_D difference of 0.5% probably results from the slightly lower Q_D value for B [hence, $F_Q(q)$ starts off with not a steep enough slope at small q]. However, in the region $2.5 \leq q \leq 5 \text{ fm}^{-1}$, F_Q does indeed scale with P_D and evidently slight differences in Q_D do not play an important role here. Later in Sec. V, in our discussion of $T_{2\pm 1}$, we come back to the quantitative relation between F_Q and P_D .

With MEC added (see Fig. 9), the relation between F_Q and P_D is scrambled somewhat. For example F_Q for Bonn is now lower than that for D4 despite the fact that B has a higher P_D . This behavior results from the potential dependence of the MEC. The MEC account for $\sim 10\%$ or more in the region $2 \text{ fm}^{-1} \leq q \leq 5 \text{ fm}^{-1}$ and are quite dependent on the potential. To be exact, they depend almost exclusively on p_* and not on P_D , with softer potentials (larger p_*) giving a larger MEC contribution. Now that F_Q has a contribution (the MEC) strongly dependent on p_* , but not on P_D , means that F_Q is no longer an exclusive measure of P_D . Furthermore, the MEC (and also its model dependence) is comparable to the differences in F_Q between different potentials.

Figure 10 indicates the corrections to F_C and F_Q due to the energy dependence of the Bonn potential. The curves indicate results for the impulse approximation (IA), the inclusion of the energy-dependent correction (with renormalization) of Eq. (8) ($\text{IA} + \partial V/\partial E$), and finally with the inclusion of MEC also ($\text{IA} + \partial V/\partial E + \text{MEC}$). Generally the $\partial V/\partial E$ effect is larger than the MEC contribution for F_C and smaller for F_Q , except that as q increases, the $\partial V/\partial E$ term cancels more and more of the MEC effect in F_Q .

We do not discuss in detail the behavior of F_M . Its features are similar to F_C for low q [owing to the common $I_{000}(q/2)$ contribution, see Eq. (3)], and the pair MEC are relatively small. However, other MEC are presumably important and we do not calculate these. The magnetic form factor itself only gives a small contribution (at nonbackward angles) to the observable quantities $A(q)$, and T_{20} for $q \leq 5 \text{ fm}^{-1}$. For $T_{2\pm 1}$ and $T_{2\pm 2}$, F_M plays an important role, but the fact that it can be measured independently by backward angle cross section means that we can divorce its role from that of F_C and F_Q in the tensor polarization

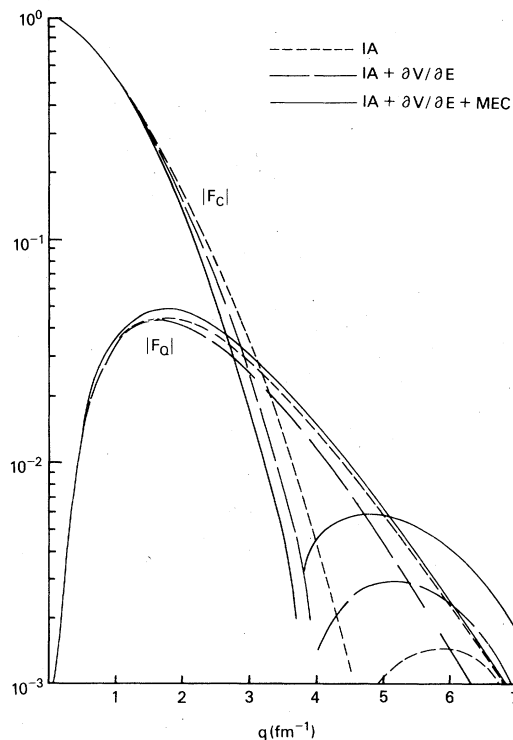


FIG. 10. $F_C(q)$ and $F_Q(q)$ for the Bonn potential in the impulse approximation (IA), with the $\partial V/\partial E$ correction of Eq. (8) ($\text{IA} + \partial V/\partial E$) and with MEC ($\text{IA} + \partial V/\partial E + \text{MEC}$).

quantities. The next section considers the role of the above observables in distinguishing $N-N$ potential models.

V. ELECTRON-DEUTERON SCATTERING OBSERVABLES

How do the changes in F_C , F_Q noted in the previous section influence the observable quantities [namely $A(q)$, T_{20} , and $T_{2\pm 1}$]? What is the role of the MEC? These are the questions addressed in this section.

Figure 11 illustrates $[A(q)]^{1/2}$ for the various potentials in the IA along with the experimental data. Up to $q \approx 4 \text{ fm}^{-1}$ $A(q)$, for the potentials in Fig. 11(a), primarily seems to distinguish the different off-shell behaviors, but not different P_D values. Up to this point the data favors the potentials with $p_* \approx 2 \text{ fm}^{-1}$. Past this point, where $F_Q(q)$ dominates and washes out the diffraction structure, $A(q)$ depends more strongly on F_Q and hence on the deuteron d wave. The data is more uncertain in this region and it is difficult to say what it implies about the deuteron wave function. Figure 11(b) demonstrates the basic difficulty in using $A(q)$ alone to distinguish potential properties: Potentials that yield significantly different off-shell and tensor force properties (such as Paris and

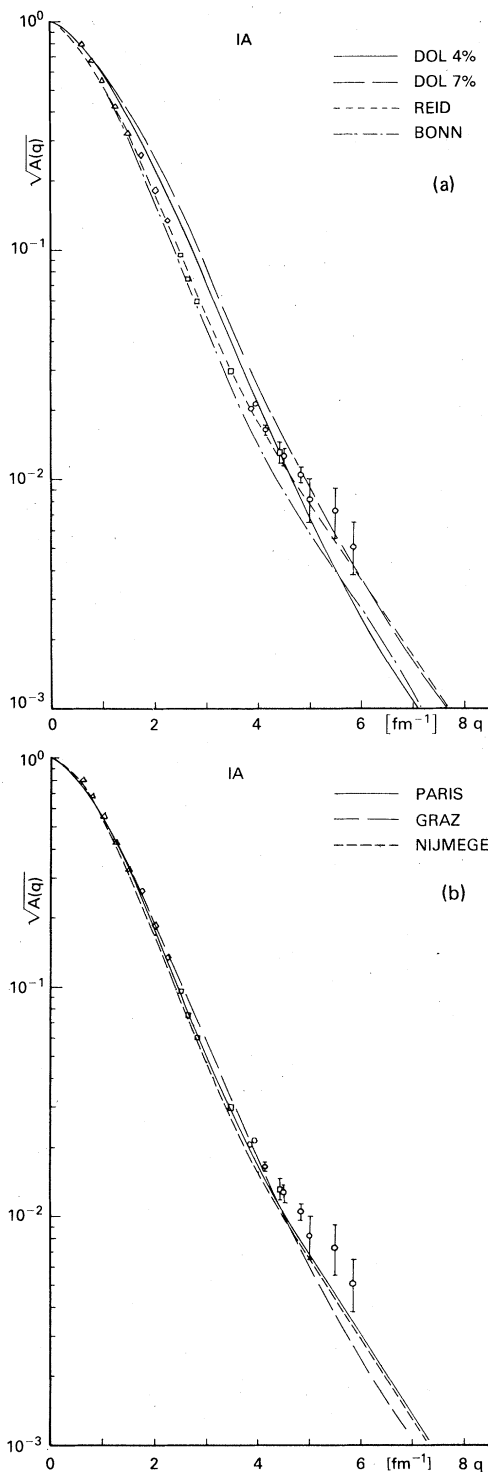


FIG. 11. $[A(q)]^{1/2}$ in the impulse approximation (a) for the potentials in Fig. 1(a) and (b) for the potentials in Fig. 1(b). The experimental points are taken from (also see Ref. 35): \circ Elias *et al.* (Ref. 35); \square C. D. Buchanan and M. R. Yearian, *Phys. Rev. Lett.* **15**, 303 (1965); \diamond D. Benaksas, D. Drickey, and L. N. Hand, *ibid.* **13**, 353 (1964); \triangle D. Drickey and L. N. Hand, *ibid.* **9**, 521 (1964).

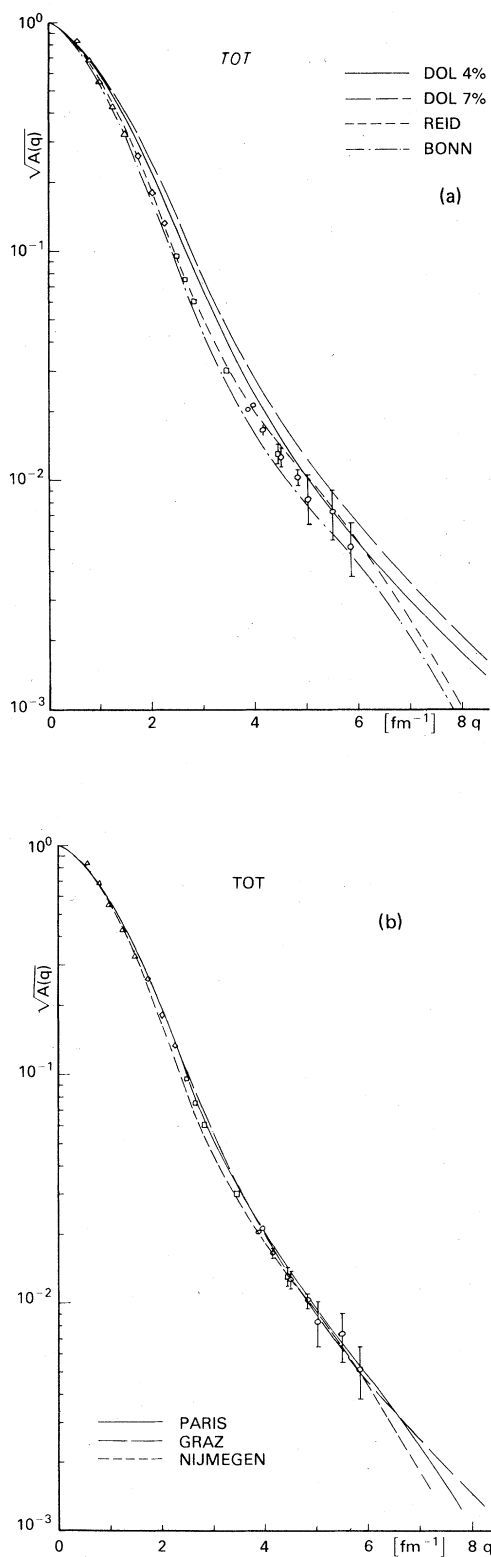


FIG. 12. $[A(q)]^{1/2}$ with MEC included (a) for the potentials in Fig. 1(a) and (b) for the potentials in Fig. 1(b). The experimental data are the same as in Fig. 11.

Nijmegen versus Graz) can give nearly the same $A(q)$ values, and also values in agreement with experiment. This occurs because $A(q)$ only measures the combination $F_C^2 + \frac{8}{9}\eta^2 F_Q^2$ and the differences in F_Q between G and P (or N) evidently cancel out the differences in F_C in this expression. When the MEC (Fig. 12) are added, the above situation with regard to $A(q)$ does not qualitatively change. With the MEC, five of the seven potentials (i.e., all except D4 and D7) give very good fits to the data all the way up to $q = 6 \text{ fm}^{-1}$. On the other hand, the $A(q)$ data still does not distinguish different P_D values very well, or simultaneous changes in F_C and F_Q (or p_+ and P_D); e.g., $A(q)$ (Paris) $\approx A(q)$ (Graz) \approx data. Obviously, different combinations of F_C and F_Q need to be measured, which can be accomplished with tensor polarization.

Figure 13 gives $[A(q)]^{1/2}$ for the Bonn potential with the effects of the $\partial V/\partial E$ [Eq. (8)], and MEC corrections. The energy-dependence correction lowers the prediction of $[A(q)]^{1/2}$ below the data for $q \leq 3.5 \text{ fm}^{-1}$, but for larger q the MEC dominates, bringing the Bonn potential in agreement with experiment. At any rate, the energy dependence does have an appreciable influence.

Figure 14 illustrates T_{20} for the different poten-

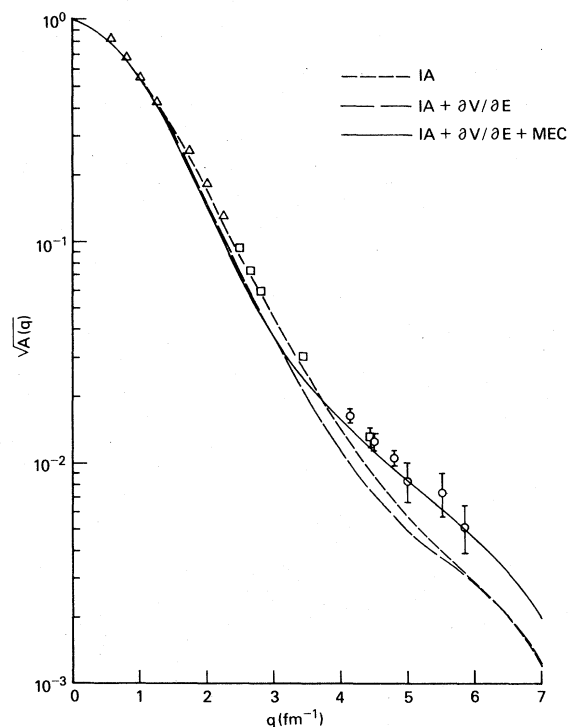


FIG. 13. $[A(q)]^{1/2}$ for the Bonn potential in the impulse approximation, with the $\partial V/\partial E$ correction of Eq. (8), and with MEC. Labels same as Fig. 10.

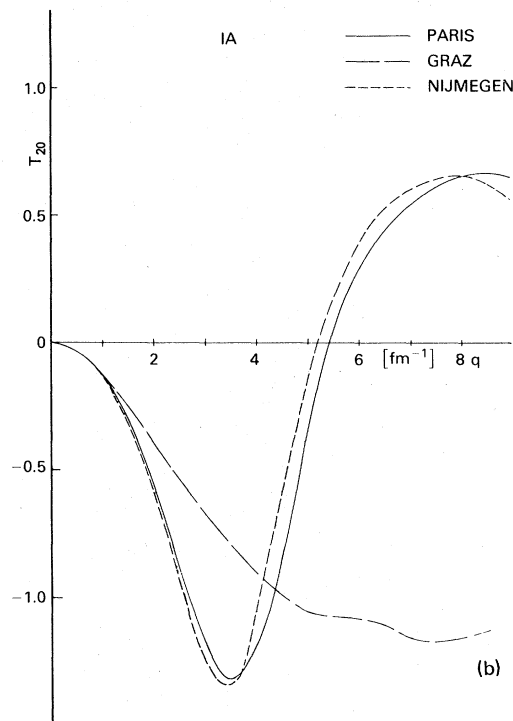
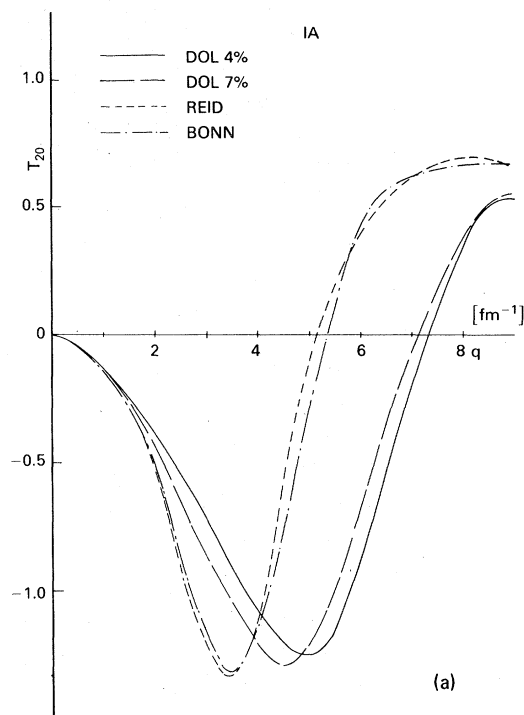


FIG. 14. T_{20} at $\theta = 0$ in the impulse approximation (a) for the potentials in Fig. 1(a) and (b) for the potentials in Fig. 1(b).

tials (at $\theta=0^\circ$) in the IA. The tensor polarization T_{20} mainly senses differences in the s -wave off-shell behavior (i.e., p_+), with perhaps a residual but small dependence on P_D . The fact that the dependence on P_D is small is surprising since F_Q would seem to dominate the expression in the numerator of Eq. (4a) for T_{20} . The zero in T_{20} occurs at a higher value of q than it does in $F_C(q)$. To get a zero, F_C must be negative enough so that the $\frac{2}{3}\eta F_C F_Q$ term in Eq. (4a) cancels out the positive contributions of the $\frac{2}{3}\eta F_Q^2 + \frac{2}{3}\eta F_M^2 [\frac{1}{2} + (1 + \eta)\tan^2(\theta/2)]$ term. Therefore the so-called "high energy component" of the s -wave deuteron wave function (or of the deuteron F_C) is involved. On the other hand, T_{20} does not distinguish different P_{HE} values as well as one might have hoped (compare B and RSC for $q \geq 5 \text{ fm}^{-1}$). Note that one need not go up to $q \approx 5 \text{ fm}^{-1}$ to distinguish different off-shell behaviors (i.e., p_+ values). Significant differences occur even by $q \approx 2 \text{ fm}^{-1}$ (around 20%) and increase greatly for larger q^2 . Conveniently for experimental measurements, differences are quite large, even percentagewise, where T_{20} has its maximum values. Also, the electron energies involved are not so high as to be unavailable at the Bates-MIT or Saclay accelerators. For $q \approx 3 \text{ fm}^{-1}$ and $\theta=30^\circ$ the needed electron energy is about 1200 MeV. However, for $q \approx 3 \text{ fm}^{-1}$ and $\theta=90^\circ$ the needed T_{elec} is only about 460 MeV. Up to 90° , T_{20} is virtually angle independent but decreases for larger angles (and F_M becomes more important). So a measurement of T_{20} at $q \approx 3 \text{ fm}^{-1}$, $\theta \approx 90^\circ$ appears quite useful and feasible. Inclusion of MEC (Fig. 15) narrows somewhat the model dependence of T_{20} , decreases the values of q^2 at which $T_{20}=0$, and narrows the peak for all potentials. The maximum value of T_{20} , however, is not greatly affected. Still, T_{20} senses the difference between the p_+ values of different potentials with $q \geq 2 \text{ fm}^{-1}$ being the best region to test the off-shell behavior. The MEC are important and need to be carefully considered before "extracting" the off-shell behavior from possible T_{20} measurements. Figure 15(b) confirms that even with MEC, T_{20} still distinguishes very well different potentials (like Graz and Paris) that give essentially the same $A(q)$. The presence of MEC, however, renders even more difficult the determination of P_{HE} .

Figure 16 shows T_{21} at $\theta=90^\circ$ in the IA and also with MEC for the potentials studied. The features are qualitatively similar (to within a sign) and the comparisons between potentials are similar, to the T_{20} calculations. The link is the (qualitatively) similar behaviors of F_C and F_M : The combination $F_M \cdot F_Q$ occurs in T_{21} , while the combination $F_C \cdot F_Q$ occurs in T_{20} [see Eqs. (4a), (4b)]. Both

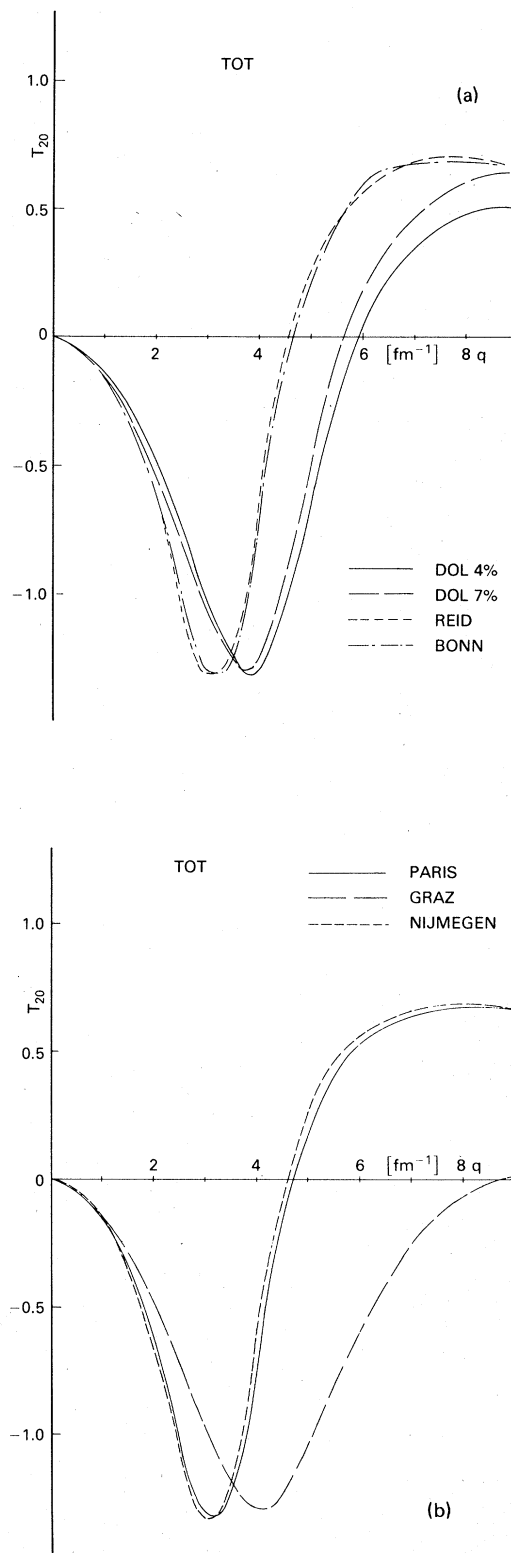


FIG. 15. T_{20} at $\theta=0$ with MEC included (a) for the potentials of Fig. 1(a) and (b) for the potentials in Fig. 1(b).

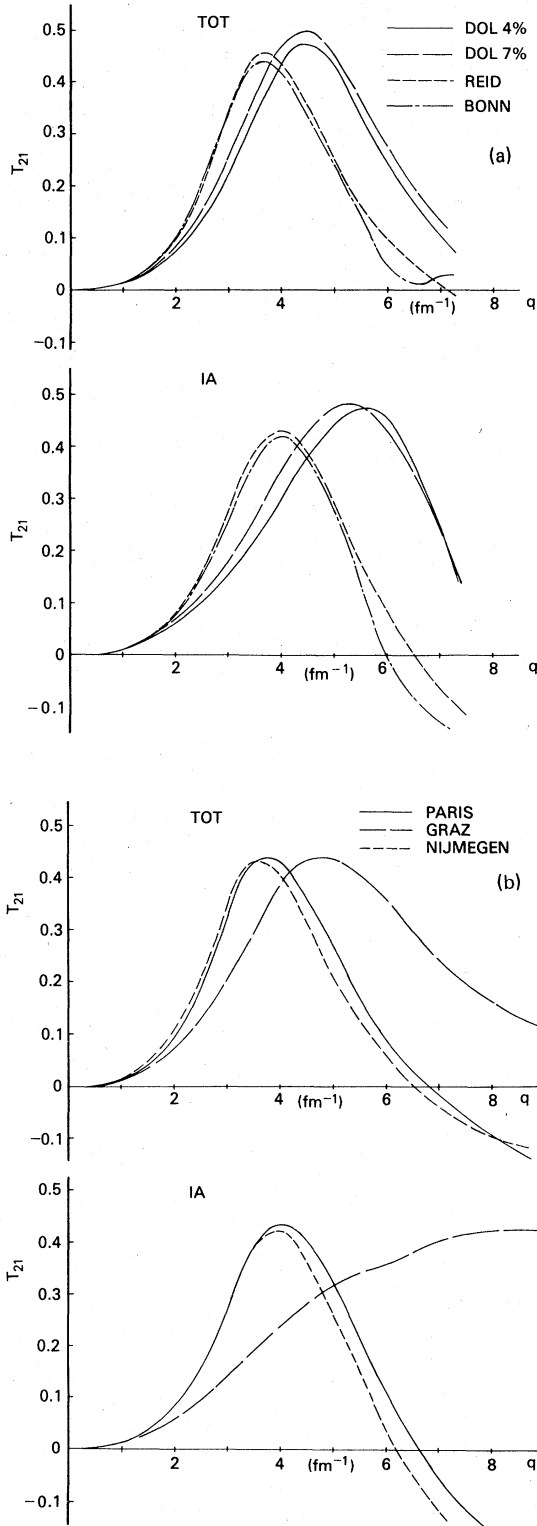


FIG. 16. T_{21} at $\theta = 90^\circ$ in the impulse approximation (lower graph) and with MEC included (upper graph) (a) for the potentials in Fig. 1(a) and (b) for the potentials in Fig. 1(b).

the position of the peak value of T_{21} and that at which T_{21} goes through zero are larger than the corresponding q values in T_{20} . The peak position is shifted to larger q because of the kinematic factors in Eq. (4b). The zero is associated with the zero in $F_M(q)$ which occurs at much larger q than the zero in $F_C(q)$.² The magnitudes are a factor of 2 or 3 lower than in T_{20} , and measurements in the region $q \geq 3 \text{ fm}^{-1}$ are needed to be useful as opposed to $q \geq 2 \text{ fm}^{-1}$ for T_{20} . As a function of θ , $T_{2\pm 1}$ (at $q \approx 3 \text{ fm}^{-1}$) maximizes at about 120° . The following table tells the relevant electron energies for $q = 3, 4 \text{ fm}^{-1}$, $\theta = 90^\circ, 120^\circ$.

	$T_{\text{elec}}(\text{MeV})$	
	$\theta = 90^\circ$	$\theta = 120^\circ$
3 fm^{-1}	461	351
4 fm^{-1}	631	487

Again, experimental measurements in the important region are feasible. Again (as with T_{20}) MEC are important to include in the analysis.

Figure 17 shows the influence of the $\partial V/\partial E$ term for the Bonn potential in predicting T_{20} and T_{21} . Its influence is fairly small on both quantities for $q < 3 \text{ fm}^{-1}$, but becomes quickly dominant (over MEC) for larger values of q . So large is its in-

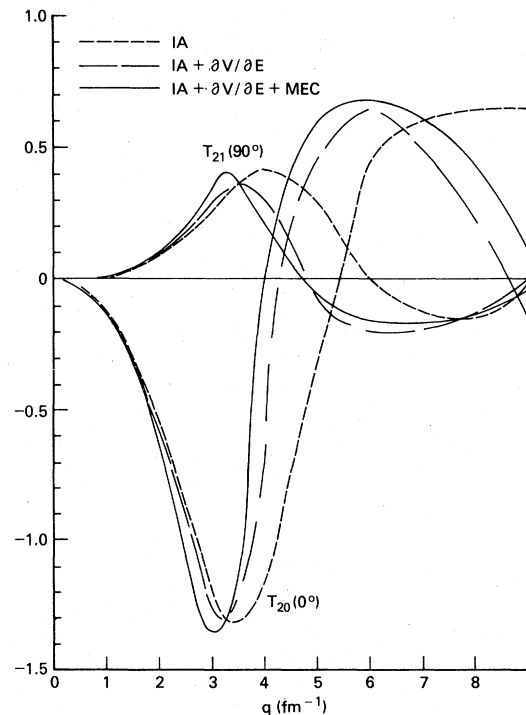


FIG. 17. T_{20} and T_{21} for the Bonn potential in the impulse approximation, with the $\partial V/\partial E$ correction of Eq. (8), and with MEC. Labels same as Fig. 10.

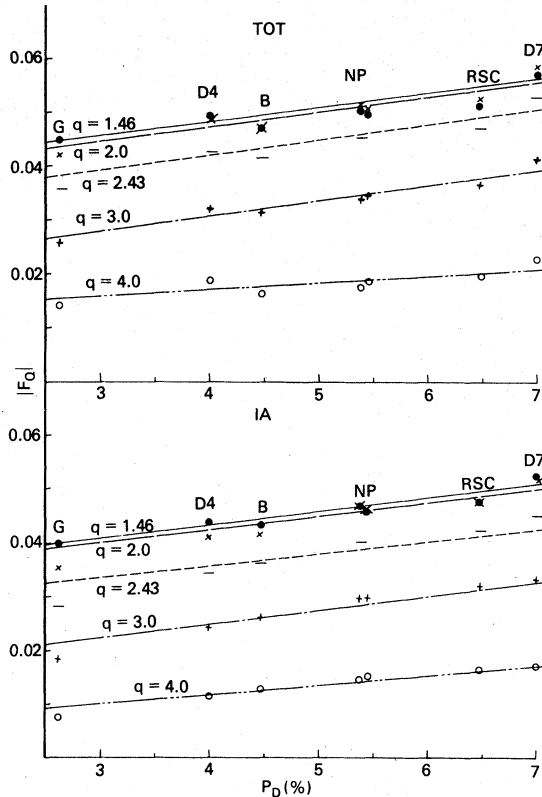


FIG. 18. $F_Q(q)$ versus P_D for several q values. Data points represent the F_Q values for each potential at a given q , while the lines indicate an approximate linear relation between F_Q and P_D at each q value.

fluence for $q \gtrsim 3.5 \text{ fm}^{-1}$ that one could be tempted to say that measurements of T_{20} (or T_{21}) for $q \gtrsim 3.5 \text{ fm}^{-1}$ could help determine the role of energy dependence in the N - N force.

The main virtue in measuring $T_{2\pm 1}$ is not directly to compare potentials (T_{20} would be better for that because T_{20} is larger with qualitatively similar features to $T_{2\pm 1}$) but to obtain a clear determination of F_Q by dividing through by an experimentally known F_M and multiplying by the also known N [$N = (d\sigma/d\Omega) / (d\sigma/d\Omega_{\text{MOTT}})$] [see Eq. (1)]. In turn, F_Q is closely related to the d wave of the deuteron and to P_D . Since F_Q is now an essentially measurable quantity, how closely is it related to P_D ? How does this relation change if MEC corrections are included in F_Q ? Figure 18 indicates $F_Q(q)$, at various values of q , for each potential versus its P_D value. The bottom graph includes no MEC while the top graph includes the pair current. In the IA the relation between F_Q and P_D is approximately linear (indicated by a straight line for each q value) with a small amount of scatter. This scatter is smaller at $q = 3$ or 4 fm^{-1} than at $q = 1.46$ or 2 fm^{-1} . This is fortunate because $T_{2\pm 1}$

has its largest values at $q \approx 4 \text{ fm}^{-1}$. The implication is that a precise measurement of $T_{2\pm 1}$ at $q = 3$ or 4 fm^{-1} (and of F_M , N as well) could fix P_D to within small limits (about to within 0.2% in the P_D value). However, when the MEC are included, more scatter develops in this relationship (see graph marked TOT). The scatter is again less at $q = 3$ or 4 fm^{-1} than for lower q . This scatter occurs because the MEC are model dependent, but depend on the s -wave behavior, not on P_D . Using the curve marked $q = 4.0$ we can judge by the slope and the scatter that even a precise measurement of F_Q (by measuring $T_{2\pm 1}$) would leave P_D uncertain to about 1%. Of course the final uncertainty would be larger due to experimental error (here a 10% experimental uncertainty implies about a 0.6% uncertainty in P_D). Also the $\partial V/\partial E$ correction could upset the relation for energy-dependent potentials. The fact that the MEC prevents a precise determination of P_D reflects the statements of Amado⁴⁸ and Friar⁴⁹ that P_D partially depends on the high momentum components and are hence dynamically linked to MEC and relativistic effects and is therefore "immeasurable." On the positive side, if one employs T_{20} measurements to fix the off-shell behavior, this could also fix the pair MEC correction and eliminate most of the scatter in Fig. 18 in the F_Q - P_D relationship. More precisely it would eliminate most of the scatter in the $F_Q(\text{TOT})$ - $F_Q(\text{IA})$ relationship. Then the $T_{2\pm 1}$ measurement would then again be very useful in extracting $F_Q(\text{IA})$ or perhaps P_D . Finally, the importance of the MEC is indicated by the fact that the MEC corrections to F_Q are comparable to (or larger than) the differences in F_Q between different potentials.

VI. CONCLUSIONS

The preceding sections have shown how electron-deuteron scattering and polarization experiments can help determine two major uncertainties in the N - N interaction—the tensor force strength and off-shell behavior. Whereas cross-section measurements, which determine $A(q)$, cannot separately distinguish the charge and quadrupole form factors (F_C and F_Q) between different potential models, the tensor polarization quantities T_{20} and $T_{2\pm 1}$ can. The tensor polarization T_{20} primarily distinguishes potentials with different s -wave off-shell behavior, i.e., with different F_C values, while $T_{2\pm 1}$ can be employed, as discussed in Secs. II and V, to determine F_Q and the tensor force strength. In addition, because of the contributions to the em operators for energy-dependent potentials, tensor polarization could be useful in exploring the possible energy dependence of

the N - N force. One main point is that the measurements that can readily distinguish different potential models involve neither measurements at very high q or very large electron energies. T_{20} should be measured at $2 \text{ fm}^{-1} \lesssim q \lesssim 5 \text{ fm}^{-1}$, $\theta \lesssim 90^\circ$ which implies T_{elec} (for $\theta = 90^\circ$) of 300 to 800 MeV. For $T_{2\pm 1}$, $q = 3$ to 6 fm^{-1} , $\theta \approx 120^\circ$ would be most propitious, which implies $T_{\text{elec}} \approx 400$ to 900 MeV. In either case the tensor polarizations are near their maximum values (~ 1 for T_{20} , ~ 0.5 for $T_{2\pm 1}$). In the case for T_{20} we would be looking for 20–100% effects, while in $T_{2\pm 1}$ we are looking for 10% effects (i.e., to determine F_Q to 10%). These types of experiments should be feasible at existing facilities.

In the intermediate momentum transfer region ($2 \text{ fm}^{-1} \lesssim q \lesssim 5 \text{ fm}^{-1}$) of interest, the pair MEC corrections are important enough that it would be unrealistic to extract potential properties without them. Therefore, a good description of the OPE

currents is necessary in analyzing these possible tensor polarization experiments. If more correct MEC calculations do not either swamp or compensate the potential dependence of tensor polarization quantities, these experiments appear to be good ways to learn about the N - N force. Finally, wave functions with isobar components should be employed in tensor polarization calculations to determine how these experiments may also detect the Δ - Δ component of the deuteron wave function.

ACKNOWLEDGMENTS

We are grateful to Professor W. Haerberli for suggesting calculations of T_{21} and T_{22} . We thank Professor K. Holinde, Professor J. J. de Swart, and Professor R. Vinh Mau for sending us their deuteron wave functions. This work was partly supported by Fonds zur Förderung der wissenschaftlichen Forschung; Project 2882. The calculations were performed at the RZ Graz.

*Present address: Code 6655, Naval Research Laboratory, Washington, D. C. 20375.

¹J. S. Levinger, in *Springer Tracts in Modern Physics*, edited by G. Höhler (Springer, Berlin, 1974), Vol. 71, p. 88; M. J. Moravcsik and P. Gosh, *Phys. Rev. Lett.* **32**, 321 (1974).

²L. Mathelitsch and H. F. K. Zingl, *Nuovo Cimento* **44A**, 81 (1977); *Phys. Lett.* **69B**, 134 (1977).

³T. Hamada and I. D. Johnston, *Nucl. Phys.* **34**, 382 (1962).

⁴R. V. Reid, Jr., *Ann. Phys. (N.Y.)* **50**, 411 (1968).

⁵R. de Tourreil and D. W. L. Sprung, *Nucl. Phys.* **A201**, 193 (1973).

⁶F. Tabakin, *Ann. Phys. (N.Y.)* **30**, 51 (1964); F. Tabakin and K. T. R. Davies, *Phys. Rev.* **150**, 793 (1966); M. Haftel and F. Tabakin, *Nucl. Phys.* **A158**, 1 (1970).

⁷L. Crepinsek, H. Oberhammer, W. Plessas, and H. Zingl, *Acta Phys. Austriaca* **39**, 345 (1974); L. Crepinsek, C. B. Lang, H. Oberhammer, W. Plessas, and H. Zingl, *ibid.* **42**, 139 (1974).

⁸P. Doleschall, *Nucl. Phys.* **A201**, 264 (1973) and private communication.

⁹D. W. L. Sprung, in *Few Body Problems in Nuclear and Particle Physics*, edited by R. J. Slobodrian, B. Cujek, and K. Ramavataram (Les Presses De L'Université Laval, Quebec, 1975), p. 475.

¹⁰For example: M. H. MacGregor, R. A. Arndt, and R. M. Wright, *Phys. Rev.* **182**, 1714 (1969); R. A. Arndt, R. H. Hackman, and L. D. Roper, *Phys. Rev. C* **15**, 1002 (1977); R. A. Bryan, in *Lecture Notes in Physics*, Vol. 87, edited by H. Zingl, M. Haftel, and H. Zankel (Springer, Berlin, 1978), p. 2.

¹¹F. Coester, S. Cohen, B. Day, and C. M. Vincent, *Phys. Rev. C* **1**, 769 (1970); M. I. Haftel and F. Tabakin, *Phys. Rev. C* **2**, 921 (1971).

¹²E. P. Harper, Y. E. Kim, and A. Tubis, *Phys. Rev. C* **6**, 1601 (1972); P. U. Sauer and J. A. Tjon, *Nucl. Phys.* **A216**, 541 (1973).

¹³N. J. McGurk and H. Fiedeldey, *Nucl. Phys.* **A281**, 310 (1977).

¹⁴M. Lacombe, B. Loiseau, J. M. Richard, R. Vinh Mau, P. Pires, and R. de Tourreil, *Phys. Rev. D* **12**, 1495 (1975). We indicate this potential by Paris (75), not to be confused with the 1978 version of the Paris potential (Ref. 33) we consider later in this paper.

¹⁵K. Holinde and R. Machleidt, *Nucl. Phys.* **A256**, 479 (1976). The potential referred to here is $\overline{\text{HM2}}$, not to be confused with the z -dependent potential (Ref. 32) used later in this paper.

¹⁶V. Z. Jankus, *Phys. Rev.* **102**, 1586 (1956); J. E. Elias, J. I. Friedman, G. C. Hartmann, H. W. Kendall, P. N. Kirk, M. R. Sogard, L. P. Van Speybroek, and J. K. de Pagter, *ibid.* **177**, 2075 (1969).

¹⁷R. Hofstadter, *Annu. Rev. Nucl. Sci.* **7**, 231 (1957).

¹⁸M. I. Haftel and W. M. Kloet, *Phys. Rev. C* **15**, 404 (1977).

¹⁹D. Schildknecht, *Phys. Lett.* **10**, 254 (1964); M. Gourdin and C. A. Piketty, *Nuovo Cimento* **32**, 1137 (1964).

²⁰J. Hockert and A. D. Jackson, *Phys. Lett.* **58B**, 387 (1975).

²¹L. J. Allen and H. Fiedeldey, in *Lecture Notes in Physics*, edited by H. Zingl, M. Haftel, and H. Zankel (Springer, Berlin, 1978), Vol. 82, p. 57; E. Hadjimichael, E. L. Lomon, and W. Turchinets, Report No. CTP 728.

²²F. Coester and A. Ostebee, *Phys. Rev. C* **11**, 1836 (1975).

²³J. Mougey, in *Lecture Notes in Physics*, edited by H. Arenhövel and D. Drechsel (Springer, Berlin, 1979), Vol. 105, p. 124.

²⁴We shall use the term "off-shell" behavior to refer to the momentum distribution of the s -wave deuteron wave function. By the dominance of the deuteron pole in the low energy off-shell ${}^3S_1 + {}^3D_1 N-N$ T matrix, the off-shell momentum dependence (even at high momenta) of the ${}^3S_1 - {}^3S_1$ T matrix (or of the 3S_1 -half shell func-

- tion) is given very well by the deuteron momentum space wave function (see Lvinger (Ref. 1) for example). Therefore the momentum space wave function is much more closely related to the off-shell behavior than to phase shifts or on-shell behavior.
- ²⁵*Polarization Phenomena in Nuclear Reactions*, edited by H. H. Barschall and W. Haerberli (The University of Wisconsin Press, Madison, 1971).
- ²⁶M. Gari and H. Hyuga, Nucl. Phys. **A264**, 409 (1976).
- ²⁷M. Gari and H. Hyuga, Z. Phys. **A277**, 291 (1976); H. Hyuga and M. Gari, Nucl. Phys. **A274**, 333 (1976).
- ²⁸D. W. L. Sprung and K. S. Rao, Phys. Lett. **53B**, 397 (1976).
- ²⁹F. Gross, in *Proceedings of the 7th International Conference on High Energy Physics and Nuclear Structure*, edited by M. Locher (Birkhäuser, Basel, 1978), p. 329.
- ³⁰H. Arenhövel, Z. Phys. **A275**, 189 (1975).
- ³¹H. F. K. Zingl, Acta Phys. Austriaca **22**, 256 (1966); J. L. Friar, Phys. Rev. C **12**, 695 (1975).
- ³²K. Kotthoff, K. Holinde, R. Machleidt, and D. Schütte, Nucl. Phys. **A242**, 429 (1975).
- ³³M. Lacombe, B. Loiseau, J. M. Richard, R. Vinh Mau, J. Cote, P. Pires, and R. de Tournreill, Report No. IPNO/TH 78-46.
- ³⁴M. M. Nagels, T. A. Rijken, and J. J. de Swart, in *Lecture Notes in Physics*, edited by H. Zingl, M. Haftel, and H. Zankel (Springer, Berlin, 1978), Vol. 82, p. 17.
- ³⁵Elias *et al.* (Ref. 16) give a rather complete survey of the experimental data including references to earlier measurements. Arnold *et al.* [Phys. Rev. Lett. **35**, 776 (1975)] have measured $A(q)$ at a very large q^2 , but that is beyond the q^2 region considered in this work.
- ³⁶M. Haftel, L. Mathelitsch, and H. Zingl, in *Proceedings of the International Conference on Nuclear Physics with Electromagnetic Interactions*, Mainz, 1979 (unpublished).
- ³⁷M. I. Haftel and F. Tabakin, Phys. Rev. C **2**, 921 (1971).
- ³⁸M. I. Haftel, Phys. Rev. C **7**, 80 (1973).
- ³⁹H. F. K. Zingl, L. Mathelitsch, and M. I. Haftel, Acta Phys. Austriaca, 1980.
- ⁴⁰I. R. Afnan and J. M. Read, Phys. Rev. C **8**, 1294 (1973).
- ⁴¹I. R. Afnan, D. M. Clement, and F. J. D. Serduke, Nucl. Phys. **A170**, 625 (1971).
- ⁴²F. Iachello, A. D. Jackson, and A. Landé, Phys. Lett. **43B**, 191 (1973).
- ⁴³F. Gross, in *Lecture Notes in Physics*, edited by H. Zingl, M. Haftel, and H. Zankel (Springer, Berlin, 1978), Vol. 82, p. 46.
- ⁴⁴Reference 26 does not display separately the ρ - ω and pair contribution for the magnetic form factor, just the total. The present calculation finds the pair contribution to $F_M(q)$ to be small.
- ⁴⁵The expression in Ref. 26 [their Eq. (5.10)] is incorrect for $F_M(q)$. The prescription should be
- $$+ \frac{g_{\rho NN} g_{\pi NN} g_{\rho\pi\pi} \gamma}{4m_N^2 m_\rho} \rightarrow + \frac{g_{\pi NN}^2 G_M^S(q)}{32m_N^5},$$
- as can be verified from their development from Eqs. (3.2b) and (3.4b) once one realizes that a factor ie (not c) should appear in Eq. (3.2b). Furthermore, in contradiction to these authors, their Eq. (3.4b) is consistent with Jackson *et al.* (Ref. 47) aside from their inclusion of the πNN vertex function. With these corrections our Eq. (6c) is consistent with both Ref. 26 and Jackson *et al.*, with our F_M being defined as twice the F_M of Ref. 26 and twice the G_M of Jackson *et al.*
- ⁴⁶J. A. Tjon and M. J. Zuilhof, Phys. Lett. **84B**, 31 (1979).
- ⁴⁷A. D. Jackson, A. Lande, and D. O. Riska, Phys. Lett. **55B**, 23 (1975).
- ⁴⁸R. D. Amado, Phys. Rev. C **19**, 1473 (1979).
- ⁴⁹J. L. Friar, in *Lecture Notes in Physics*, edited by H. Arenhövel and D. Drechsel (Springer, Berlin, 1979), Vol. 108, p. 445.